Ecosystems
https://doi.org/10.1007/s10021-022-00793-2

ECOSYSTEMS

25TH ANNIVERSARY PAPER

The Interplay of the Tree and Stand-Level Processes Mediate Drought-Induced Forest Dieback: Evidence from Complementary Remote Sensing and Tree-Ring Approaches

Daniel Moreno-Fernández,[1,2]* J. Julio Camarero,[3] Mariano García,[4] Emily R. Lines,[5] Jesús Sánchez-Dávila,[1] Julián Tijerín,[1] Cristina Valeriano,[3] Alba Viana-Soto,[4] Miguel Á. Zavala,[1] and Paloma Ruiz-Benito[1,4]

[1]*Forest Ecology and Restoration Group, Departamento de Ciencias de la Vida, Universidad de Alcalá, Edificio Ciencias, Campus Universitario, 28871 Alcalá de Henares, Madrid, Spain;* [2]*Departamento de Sistemas y Recursos Naturales, Universidad Politécnica de Madrid, Calle de José Antonio Novais, 10, 28040 Madrid, Spain;* [3]*Instituto Pirenaico de Ecología (IPE-CSIC), Avda. Montañana 1005, 50192 Zaragoza, Spain;* [4]*Departamento de Geología, Geografía y Medio Ambiente, Environmental Remote Sensing Research Group, Universidad de Alcalá, Calle Colegios 2, 28801 Alcalá de Henares, Spain;* [5]*Department of Geography, University of Cambridge, Downing Place, Cambridge CB2 3EN, UK*

Abstract

Drought-induced forest dieback can lead to a tipping point in community dominance, but the coupled response at the tree and stand-level response has not been properly addressed. New spatially and temporally integrated monitoring approaches that target different biological organization levels are needed. Here, we compared the temporal responses of dendrochronological and spectral indices from 1984 to 2020 at both tree and stand levels, respectively, of a drought-prone Mediterranean *Pinus pinea* forest currently suffering strong dieback. We test the influence of climate on temporal patterns of tree radial growth, greenness and wetness spectral indices; and we address the influence of major drought episodes on resilience metrics. Tree-ring data and spectral indices followed different spatio-temporal patterns over the study period (1984–2020). Combined information from tree growth and spectral trajectories suggests that a reduction in tree density during the mid-1990s could have promoted tree growth and reduced dieback risk. Additionally, over the last decade, extreme and recurrent droughts have resulted in crown defoliation greater than 40% in most plots since 2019. We found that tree growth

Received 14 March 2022; accepted 18 September 2022

Supplementary Information: The online version contains supplementary material available at https://doi.org/10.1007/s10021-022-00793-2.

Author's contribution: DM-F contributed to conceptualization, gathering field data, statistical analysis, writing—original draft preparation; JJC contributed to conceptualization, writing—reviewing editing, funding acquisition; MG contributed to conceptualization, gathering field data, writing—reviewing editing, funding acquisition; ERL contributed to gathering field data, revising and editing; JS-D contributed to gathering field data, revising and editing; JT contributed to gathering field data, writing—reviewing editing; CV contributed to processing of tree-ring data, writing—reviewing editing; AV-S contributed to processing of RS data, writing—reviewing editing; MAZ contributed to conceptualization, writing—reviewing editing, funding acquisition; PR-B contributed to conceptualization, gathering field data, writing—reviewing editing, funding acquisition.

*Corresponding author; e-mail: danielmorenofdez@gmail.com

Published online: 17 October 2022

and the greenness spectral index were positively related to annual precipitation, while the wetness index was positively related to mean annual temperature. The response to drought, however, was stronger for tree growth than for spectral indices. Our study demonstrates the value of long-term retrospective multiscale analyses including tree and stand-level scales to disentangle mechanisms triggering and driving forest dieback.

Key words: Climate change; Decline; Die-off; Mortality; Multiscale assessment; Recovery.

Highlights

- Tree growth and spectral indices decoupled during drought-triggered dieback.
- Dieback is a consequence of recurrent, severe drought events.
- Interactive tree and stand-level responses drive forest dieback.

Introduction

Climatic extremes can impact forest functioning at multiple scales and affect a wide range of processes, from tree physiology (Salmon and others 2019; Rubio-Cuadrado and others 2021) and phenology (He and others 2018), to growth (Seifert and others 2017; Abiyu and others 2018) and stand productivity (Anderegg and others 2019; Khoury and Coomes 2020). Despite increases in the magnitude and frequency of extreme events acting as one of the main drivers of forest damage and mortality (Anderegg and others 2020), low-intensity climatic events can also be a cause of forest dieback (sensu (Mueller-Dombois 1988), that is ''the unseasonal loss of crown foliage (partial or complete) of many trees of a stand'') and mortality. These events can lead to cumulative and carryover legacy effects (Franklin and others 1987; Sánchez-Pinillos and others 2021) resulting in reduced biomass (Ma and others 2012).

Climate-driven die-off and mortality events occur because the cumulative impacts of environmental variation and lead to amplified and rapid impacts at the community level, such as changes in structure, shifts in species composition or even forest collapse (Brook and others 2013; Reyer and others 2015). In addition, forest response and resilience to climatic perturbations (Lloret and others 2011) are modulated by forest structure (Bottero and others 2017; Jump and others 2017; Navarro-Cerrillo and others 2019) and composition (De Keersmaecker and others 2015; Greenwood and others 2017; Gazol and others 2018; Li and others 2021; Liu and others 2021b). Understanding the mechanisms driving forest responses to climatic extremes requires analyses of processes operating at multiple spatio-temporal scales and levels of biological organization.

At the individual level, it is generally assumed that secondary radial growth is positively related to health status (Dobbertin 2005; Camarero and others 2015b). Tree-ring width data obtained through dendrochronological techniques have been widely used to describe the resilience of radial growth in response to climatic impacts (Drobyshev and others 2021; Marqués and others 2021). Yet their capability to characterize the impacts of drought on population and community dieback processes—for example, including plant to plant interactions across several spatial scales—remains more limited, largely due to lack of data. At the stand and landscape scales, remote sensing provides temporal series of continuous observations of forest vitality (Rogers and others 2018; Buras and others 2021; Moreno-Fernández and others 2021). These observations trace aggregated vegetation responses to the environment conditions through spectral indices associated with functional processes such as photosynthesis rates (that is, greenness indices) or water content (that is, wetness indices) (Tucker 1979; Gao 1996). Spectral indices, however, aggregate multiple forest components and processes because they include canopy dominant and understory layers (Ahl and others 2006; Ryu and others 2014).

The impact, severity and magnitude of the biotic and abiotic perturbations on temporal series of tree growth and spectral indices can be quantified through the forest resilience (Lloret and others 2011), sensu the engineering resilience or the ability of a system to return to its pre-disturbance stage and the capacity to absorb change and disturbance while maintaining similar feedback dynamics (please see Bone and others (2016) and Nikinmaa and others (2020) for other definitions of forest resilience). The comparison of tree-ring data and remote sensing approaches allow us for continuous and retrospective monitoring processes key to drought-induced responses, including individual tree responses (Camarero and others 2015b), functional and structural rapid adjustments as photosynthesis and leaf shedding (Aragones and others 2019; Wu and others 2021) and water (Gao

1996), opening a new avenue to further understand long-term dynamics. Few studies, however, have addressed simultaneously the impact of drought episodes on resilience indices based on tree ring and remote sensing information (Gazol and others 2018).

Several studies have assessed the strength of the correlation between temporal series of spectral indices and tree growth data. Many of them have found positive relationships between tree and stand-data, although the strength of the association varies across biomes or species (Vicente-Serrano and others 2014, 2020; Zhou and others 2020; Castellaneta and others 2022). Mechanisms of resilience can be understood by examining different metrics of response, for example Gazol and others (2018) found that resilience to drought was more pronounced in tree-ring width than satellite-based indices, suggesting that trees may reallocate resources to photosynthesis and repair canopy damage in detriment of radial growth to alleviate the impact of a drought episode (Kannenberg and others 2019). Both tree-ring data and multispectral indices have been able to detect forest dieback before the externalization of the symptoms, this is early warning signals of forest dieback (Camarero and others 2015b; Rogers and others 2018; Moreno-Fernández and others 2021; Valeriano and others 2021). Several issues deserve to be further investigated in the use of multiscale approaches combining long-term tree and stand responses to understand drought-induced mortality (Allen and others 2015), including successive drought events, which can have critical impacts on long-term dynamics leading to abrupt responses at tree and stand levels (Navarro-Cerrillo and others 2018; Chuste and others 2020; San-José and others 2021; Yang and others 2021). Furthermore, responses to mean climate and climatic extremes can differ and be mediated by stand-level competition (Marqués and others 2021; Serra-Maluquer and others 2021). However, the importance of recurrent droughts and extreme events on both tree growth and spectral indices have not been previously assessed simultaneously (Castellaneta and others 2022).

Here, we retrospectively investigated multiscale tree and stand-level responses to drought in a Mediterranean stone pine (*Pinus pinea* L.) forest suffering a recent and pronounced dieback process. Specifically, we (i) explored the degree of coupling between tree-ring width (that is, secondary growth) and greenness and wetness spectral indices (that is, related to stand primary productivity and biomass accumulation) during drought episodes; (ii) quantified tree growth and spectral responses to climate; and (iii) investigated resilience, resistance and recovery for both tree- and stand-level processes in response to drought events. Our results provide evidence of long-term forest responses to recurrent droughts at tree and stand-level, which could be helpful to further characterize and understand complementary ecological scales.

Material and Methods

Study Area, Field Sampling and Climatic Information

The study was conducted in a *P. pinea* forest of 1500 ha, with a widespread dieback process since 2019. The forest is located in Central Spain (40.27526 N, 4.36569 W) at an altitude ranging from 500 to 850 m a.s.l. on acid soils (Figure 1). For this species, the site quality of the area is moderate (Aguirre and others 2022). Despite *P. pinea* being the main species, *Quercus ilex* L. (holm oak) and *Juniperus oxycedrus* L. (cade juniper) are also present in the midstory, and *Cistus ladanifer* L. and aromatic dwarf shrubs (Lamiaceae), such as *Salvia rosmarinus* L. and *Lavandula stoechas* Lam., complete the understory layer.

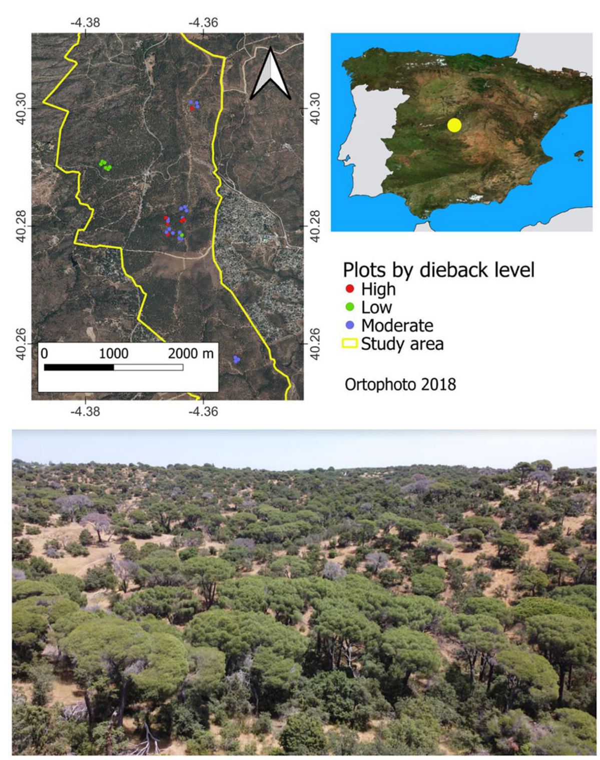

Figure 1. Location of our study area in central Spain (upper right); plots with low (green), moderate (blue) and high (red) dieback intensity within the area; and drone flight picture (June 2021. Author: Emily R. Lines).

The forest is under a continental Mediterranean climate, with a mean annual temperature of 14.2 °C and a mean annual rainfall of 568 mm. The rainfall is irregularly distributed through the year with spring (March, April and May) and autumn (September, October and November) being the wettest months. Summer months are especially warm and dry, which may result in long periods of water deficit and extreme droughts. In 2019, forest rangers reported a strong and rapid dieback process in the pine forest, which was confirmed by analyzing recent orthophotos. Likely, there were no changes in forest management or pathogens present during the period of study, so the dieback process was associated with rapidly changing climate conditions and drought stress.

We installed thirty-one 17-m-radius circular plots (that is 908 m^2), equivalent to the area of a 30 m Landsat pixel, during May–June 2021 aiming at covering the widest range of dieback. Before plot establishment, we visited the area with the forest rangers and managers and delimited areas according to dieback level. Then, we visually classified the study area into damage levels using a planet image (www.planet.com, 24/03/2021) with a spatial resolution of three meters using false color to identify the vegetation status (R/G/B as IR/R/G; see Figure S1 in Supplementary Material). Finally, we randomly established the sampling plots within each level.

We positioned the plot center with an EMLID REACH RS2 GPS receiver (Ng and others 2018) capable of sub-meter accuracy using Differential Global Positioning System techniques. Within each plot, we measured the diameter at breast height (dbh) and identified the species of each adult tree (trees with dbh $\geq$ 7.5 cm). Canopy defoliation, defined as the percentage of needle loss in a crown as compared to a reference, fully foliated tree, was evaluated at least by two observers as a proxy of forest dieback in classes of 5% following the ICP Forest Manual (ICP Forest 2016). We calculated the mean plot defoliation weighting the tree defoliation by the dbh as a proxy of crown size (Porté and others 2000; Moreno-Fernández and others 2021). Then, we classified the damage level of each plot according to their mean plot defoliation: low (defoliation < 50%), moderate (50% $\leq$ defoliation < 70%) and high (defoliation $\geq$ 70%, see Table 1).

We calculated several forest attributes including stand basal area (m^2 ha^{-1}), tree density (trees ha^{-1}) and mean tree dbh (Table 1). We used analysis of variance to assess if there were significant differences in these variables among diebacks levels, and we did not find significant relationships between the dieback level and mean tree diameter (p = 0.6977), stand density (p = 0.7693) and basal area (p = 0.0868), suggesting that the stand variables are not linked to the dieback process. Similarly, we evaluated the effect of potential soil water availability on the dieback phenomenon using the topographic wetness index and we neither found a significant relationship (p = 0.7853) between both variables. Additionally, we collected cores from approx. six pine trees per plot at 1.3 m (one core per tree) using a 5-mm Pressler increment borer aiming at reconstructing radial growth across a wide range of sizes and dieback status in each plot. We selected the trees to core considering a good coverage of tree sizes and health status, aiming at sampling at least a dead and healthy tree per plot.

Aiming to characterize the temporal variations in climatic conditions, we derived the 12-month December Standardized Evapotranspiration Index (SPEI; https://monitordesequia.csic.es/) at a 1 km^2 resolution (Vicente-Serrano and others 2017). Low values of SPEI point to a negative water cumulative balance as a function of precipitation and temperature at different time scales (Vicente-Serrano and others 2010). Years with SPEI values lower than -1 were considered as drought years, due to its classification as moderate or extreme drought (Alam and others 2017) and the reasonable cut-off for our Mediterranean data (Figure 2A). We also calculated the mean annual temperature and the cumulative annual precipitation over 1984 to 2020 (see Figure S2 in Supplementary Material) from the eight nearest climatic stations using the *meteoland* package (De Cáceres and others 2018) implemented in R 4.1.1 (R Core Team 2021).

Multispectral Image Processing

We used Google Earth Engine to access the open-access multispectral images from the Landsat archive and we derived the two following indices for the pixels that contain the center of each plot:

$$\mathrm{NDVI} = \frac{(\mathrm{NIR} - \mathrm{RED})}{(\mathrm{NIR} + \mathrm{RED})} \tag{1}$$

$$\mathrm{NDWI} = \frac{(\mathrm{NIR} - \mathrm{SWIR1})}{(\mathrm{NIR} + \mathrm{SWIR1})} \tag{2}$$

NDVI (Normalized Difference Vegetation Index) is a greenness vegetation index, that is, it is based on the estimation of absorbed photosynthetically active radiation, commonly used to assess the vegetation health status (Tucker 1979). NDWI (Normalized Difference Water Index) is a vegeta-

Table 1. Mean Values of Forest Attributes, Basal Area Increment (BAI) and Spectral Indices Including NDVI and NDWI in the Plots with Low, Moderate and High Dieback Intensity

Variable	Low	Moderate	High
No. Plots	7	18	6
Plot defoliation (%)	28.6 (7.7)	67.1 (5.0)	81.6 (5.9)
Basal area (m^2 ha^{-1})	22.7 (5.3)	19.2 (5.6)	17.1 (4.3)
Pine basal area (%)	95.8 (4.0)	90.3 (9.4)	89.9 (3.0)
Tree density (No. trees ha^{-1})	244 (64)	278 (95)	272 (98)
Mean tree diameter (cm)	31.0 (7.6)	27.1 (5.9)	25.4 (2.5)
No. cored of alive/dead trees	24/2	77/9	21/12
Timespan of cored trees	1859–2021	1807–2021	1835–2021
Age at 1.3 m (years)	106 (44)	97 (32)	107 (47)
Mean BAI correlation between trees	0.65 (0.11)	0.67 (0.12)	0.72 (0.08)
BAI (mm^2 $year^{-1}$)	1626.9 (506.0)	1075.2 (323.9)	940.5 (188.0)
NDVI	0.58 (0.02)	0.57 (0.03)	0.59 (0.04)
NDWI	0.20 (0.04)	0.17 (0.06)	0.21 (0.08)

Between brackets, the standard deviation.

tion index based on the near-infrared (NIR) and short-wave infrared (SWIR) regions and relates to the vegetation water content (Gao 1996).

For the calculation of these two spectral indices, we selected monthly and cloud-free observations from January 1984 to December 2020 and applied the topographic correction and inter-sensor harmonization. First, we normalized Tier 1 Surface Reflectance images from Landsat 5 TM, Landsat 7 ETM + datasets to Landsat 8 OLI datasets from a multilinear regression approach due to differences between spectral characteristics among sensors (Roy and others 2016). Then we applied the topographic correction SCS + C proposed by Soenen and others (2005), which is based on the Sun-Canopy- Sensor correction (Gu and Gillespie 1998), to remove the effect of the terrain slope. After applying these corrections, we generated monthly composites using a medoid selection process choosing the pixel closest to the median of the corresponding pixels among images (Flood 2013; Bright and others 2019).

We used the BEAST (Bayesian Estimator of Abrupt change, Seasonal change, and Trend; (Zhao and others 2019b)) to separate the spectral indices trend signal (*Trend*) from seasonality, that is, intra-annual variability associated with forest phenology, and noise. BEAST is an ensemble algorithm that fits individual models, measures their relative importance, and averages these individual models throughout a Bayesian framework instead of selecting a single best model. In contrast to other algorithms that derive only linear or piecewise linear trends, this routine fits linear and nonlinear trends by applying flexible basis functions (Zhao and others 2019b), so it is suitable for ecological applications where processes usually follow non-linear and complex patterns over time instead of linear or piecewise linear patterns. This approach has been previously used to discriminate plots according to their forest health status (Moreno-Fernández and others 2021). Deeper statistical details of BEAST are given in Zhao and others (2019b). This routine is implemented in the *Rbeast* package (Zhao and others 2019a) in R 4.1.1 (R Core Team 2021).

Tree-Ring Analyses

The cores were air-dried, mounted on wooden supports, and then sanded with sandpapers of successively finer grain until tree rings were visible. Samples were visually cross-dated using marker rings (Yamaguchi 1991), and tree-ring widths were measured with a 0.001 mm resolution on scanned images (Epson Expression 10000XL scanner) using the CDendro and CooRecorder software (Larsson and Larsson 2017). The visual cross-dating was further checked using the COFECHA software, which calculates shifting correlations with a mean site series (Holmes 1983). We converted the ring-width data into basal area increments (BAI, mm^2 $year^{-1}$) assuming a circular outline of stems (Visser 1995) as follows:

$$\mathrm{BAI}_t = \pi\left(r_t^2 - r_{t-1}^2\right) \quad (3)$$

where r is the tree radius while t is the year of tree-ring formation. We used BAI because it eliminates the radial growth variations associated with increasing circumference and keeps both the long

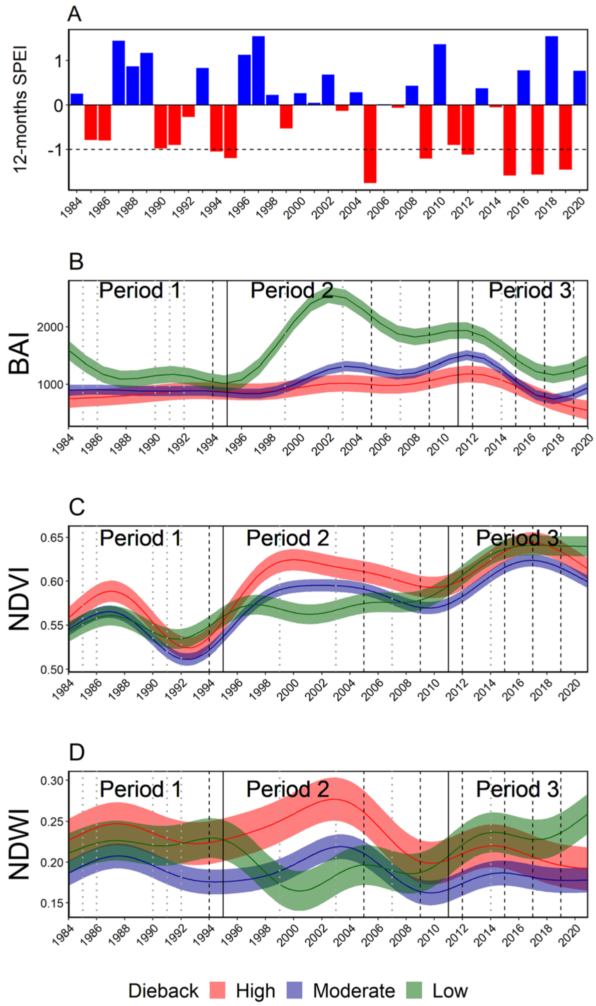

Figure 2. The 12-month December Standardized Precipitation Evapotranspiration Index (SPEI) recorded from 1984 to 2020. We considered a drought event when SPEI < −1 (**A**) and the representation of the smooth functions (Eqs. 4–5) for the basal area increment (BAI, in mm^2 $year.^{-1}$, (**B**)) and the two spectral indices (NDVI (**C**) and NDWI (**D**)) over the monitoring period (January 1984–December 2020) grouped by dieback level. The shaded areas indicate the standard errors. Solid vertical lines refer to the period delimitation (1984–1995, 1995–2011, 2011–2020, see ''Temporal trends of tree growth data and spectral indices'' section. for further information on periods), dashed black vertical lines correspond to years with SPEI < −1 and dotted gray vertical lines correspond to years with −1 ≤ SPEI < 0.

and short-term changes in tree growth (LeBlanc and others 1992). We fitted linear or exponential functions to BAI data to remove long-term BAI trends and obtained detrended BAI series by dividing observed by fitted values using the *dplR* package (Bunn 2010) in R 4.1.1 (R Core Team 2021).

It is worth noting that we cored alive and dead trees, which mainly died recently (40% during 2018–2019; Figure S3). The year of death was estimated considering the last tree ring. Despite alive trees exhibiting greater BAI than dead trees over the study period, the BAI trends followed a similar pattern (Figure S4), and, therefore, we performed the statistical analyses combining both alive and dead trees.

Temporal Trends of Tree Growth and Spectral Indices

To compare the trends of tree growth data and spectral indices, we modeled the temporal pattern of tree growth (that is, BAI) and the trend component of NDVI and NDWI (*Trend*) as a function of damage level, time, plot and tree, using additive mixed models and the R package *mgcv* (Wood 2017). Additive models allow complex and nonlinear relationships between response and predictors to be described, especially in ecological studies (Faraway 2006; Wood 2006). We proposed the following models for BAI (4) and *Trend* (5) data:

$$\mathrm{BAI}_{\mathrm{itnk}} = \mathrm{Dieback}_k + f^k(\mathrm{Time}_t) + \mathrm{Plot}_i + \mathrm{Tree}_n + \varepsilon_{\mathrm{itnk}} \tag{4}$$

$$\mathrm{Trend}_{\mathrm{imk}} = \mathrm{Dieback}_k + f^k(\mathrm{Time}_m) + \mathrm{Plot}_i + \varepsilon_{\mathrm{imk}} \tag{5}$$

where *Dieback* is a factor referred to the tree and plot damage level (k = low, moderate and high), f^k(Time) is a damage level smoother via thin plate regression splines (Wood 2003) where the smoothing variable is the *Time* in years (subfix t) for (4) and in months (subfix m) for (5). This formulation allows each dieback level to be differently shaped over the study period (Pedersen and others 2019). *Plot* and *Tree* are random effects to account for the intra-plot variability (i = 1, …, 31) and intra-tree variability (n = 1, …, 145), and ε is the error term of each plot i, time (either year t or month m) and damage level k (Zuur and others 2009). Because the data sources differed in temporal length (from 1970 to 2020 for tree growth and from 1984 to 2021 for spectral indices), the three data sets (tree growth, NDVI and NDWI) were filtered bounding the same temporal range, that is, from 1984 to 2020, to allow temporal comparisons. Temporal autocorrelation was accounted for through autoregressive structures of errors.

Relationships of Climate Condition with Tree-Ring Growth Data and Spectral Indices

We used dispersion plots and the Spearman's correlation coefficient to investigate the correlations between plot tree growth and spectral indices. In the case of tree growth, we considered the BAI chronologies for each plot as well as the detrended chronologies of BAI. We fitted polynomial (20-year long splines) to BAI data to remove BAI trends and obtained detrended BAI series by dividing observed by fitted values using the *dplR* package. In the case of the spectral indices, we averaged annual and summer (June, July and August) values for both raw and *Trend* values of both indices.

The relationships between climate conditions (temperature and precipitation) and tree growth and spectral indices between 1984 and 2020 were quantified with linear mixed models in the R package *nlme* (Pinheiro and others 2020). For tree growth, BAI was transformed as log(detrended BAI + 1) to meet the assumption of normality. We included a first-order autoregressive structure of errors to account for the temporal autocorrelation (Zuur and others 2009) and the tree id or plot id as a random intercept term. Temperature and Precipitation were centered and scaled to facilitate the interpretability of the regression coefficients and the interaction terms (Schielzeth 2010). We proposed the following model formulations:

$$\log(\mathrm{BAI}_{\mathrm{itn}} + 1) = \mathrm{Prep}_t + \mathrm{Temp}_t + \mathrm{Prep} \times \mathrm{Temp}_t + \mathrm{Plot}_i + \mathrm{Tree}_n + \varepsilon_{\mathrm{itn}} \tag{6}$$

$$\mathrm{Trend}_{\mathrm{it}} = \mathrm{Prep}_t + \mathrm{Temp}_t + \mathrm{Prep} \times \mathrm{Temp}_t + \mathrm{Plot}_i + \varepsilon_{\mathrm{it}} \tag{7}$$

Temp and *Prep* are the mean annual temperature and the cumulative annual precipitation, respectively. The climatic variables and the pairwise interaction were selected following a forward stepwise procedure via the likelihood ratio test and using the maximum likelihood (Zuur and others 2009). Finally, the restricted log-likelihood was selected to fit the final model.

Vegetation Responses to Drought: Resilience Metrics

For the drought years (SPEI < -1; Figure 2A), we evaluated the vegetation responses to drought through resistance (*Rt*), recovery (*Rc*) and resilience (*Rs*) metrics (Lloret and others 2011):

$$\mathrm{Rt} = \frac{\mathrm{Dr}}{\mathrm{PreDr}} \tag{8}$$

$$\mathrm{Rc} = \frac{\mathrm{PostDr}}{\mathrm{Dr}} \tag{9}$$

$$\mathrm{Rs} = \frac{\mathrm{PostDr}}{\mathrm{PreDr}} \tag{10}$$

where *Dr* is the growth or spectral value during a given drought event and *PreDr* and *PostDr* are the mean values of the four previous and posterior years of a given drought event (Rubio-Cuadrado and others 2018b). We evaluated the effect of the *Dieback* and drought events on the three resilience metrics using two-way repeated-measures analyses of variance for tree growth (BAI), greenness (NDVI) and wetness (NDWI) indices, that is, including 3 resilience metrics and 3 indices.

Results

Temporal Trends of Tree Growth Data and Spectral Indices

We found a significant effect of *Dieback* on tree growth ($p > 0.05$) according to the Wald test. Tree growth was greater in areas with low dieback levels (Table 1 and Figure 2B), but there were no corresponding differences for spectral indices (Table 1 and Figure 2C–D). However, the inclusion of the smoothing term $f^k(Time)$ significantly improved all models, indicating that the temporal patterns of the dieback varied over time for the three response variables studied (tree growth, NDVI and NDWI). We visually defined three temporal periods (1984–1995, 1995–2011 and 2011–2020, see Figure 2) to facilitate the interpretation of the results.

In the first period (1984–1995), tree growth and spectral indices responses overlapped for the curves of the three dieback categories (Figure 2B–D and see Figure S5 for the arithmetic mean trends for tree growth). NDVI had a local minimum in 1992–1993 that SPEI analysis suggests was preceded by dry years (Figure 2C), but this minimum was less pronounced for NDWI (Figure 2D). Following this, NDVI and NDWI increased until the dry years of 1994–1995.

In the second period (1995–2011), spectral indices had a higher value in moderate and high dieback than in areas with low dieback, whereas the opposite trend was found for BAI (see Figure 2B vs. Figure 2C–D). The smooth functions of spectral indices for the low dieback level reached minima in 2000–2001 and 2009–2010 for the three dieback levels. The 2009–2010 minimum occurred a couple of years lagged behind the reduction in tree growth in 2008.

In the third period (2011–2020), drought frequency was highest (years 2012, 2015, 2017 and 2019; Figure 2A). Tree growth had the steepest drop after the 2012 drought, regardless of dieback level, but this drought seems to have a negligible impact on spectral indices. However, we found different patterns between NDVI and NDWI trends (Figure 2C and D). The rates of initial increase and subsequent decrease were larger for NDVI than NDWI, and NDWI peaked earlier (2014) during this period than NDVI (2017). Low dieback plots showed higher values in the spectral indices through this period. Finally, spectral indices and tree growth showed a decrease from 2017 to 2019, in line with the recurrent droughts over this time period. After 2018–2019 smooth functions for the three indices increased in areas of low dieback and decreased in areas of high dieback.

Relationships of Climate Conditions with Tree Growth and Spectral Indices

We did not find significant relationships between tree growth chronologies and the annual and summer spectral indices (Spearman's correlation coefficient, $p > 0.05$, see Figure S6). The likelihood test indicated that precipitation was positively related to tree growth and NDVI, but we did not find a significant relationship with NDWI. However, the temperature was positively and significantly related to NDWI (Table 2).

Vegetation Responses to Drought: Resilience Metrics

The SPEI series revealed droughts in 1994–1995, 2005, 2009, 2012, 2015, 2017 and 2019 (Figure 2A). We found a significant effect of *Drought* on the three resilience metrics for tree growth and spectral indices whereas *Dieback* did not have a significant impact on any of the resilience components (Eqs. 9–11) according to the likelihood ratio test. *Resistance* was similar for both spectral indices over the seven studied droughts, and did not show a clear linear trend, whereas *Resistance* for tree growth displayed a decreasing trend over the study period (Figure 3A). *Resilience* followed similar patterns for the three variables (tree growth, NDVI, NDWI), with the highest values found in 1994–1995 and 2012, and the lowest in 2005, 2015 and 2017 (Figure 3B). *Recovery* displayed relatively constant values for spectral indices, while values for tree growth reached the largest *Recovery* value during the drought of 2019 (Figure 3C).

Discussion

The Interplay Between Tree and Stand Responses to 1990s Drought Underlies Current Dieback

Our results indicate that recent forest dynamics are driven by a climatic legacy. Specifically, droughts during the first period (1995 the most remarkable) triggered a divergence in trajectories of stands in our study area. Stands already displaying intense and rapid canopy dieback did not exhibit a further drop in tree growth and spectral indices during the second period (middle 1990s). Therefore, we suggest that the differential tree (tree growth) and stand responses (spectral indices) in low vs medium–high dieback were partially due to differences in 1990s droughts. The strong effect of the 1990s drought has been already reported in other Iberian forests (Pacheco and others 2018; Moreno-Fernández and others 2021). Furthermore, low dieback level showed a marked reduction in spectral indices after the 1995 drought, and a rapid increase in tree growth. The drop in spectral indices can be explained by a decrease in biomass, that is, stocking or tree density (also namely stocking or biomass release) (Ogaya and others 2015; Zhu and Liu 2015), and therefore a reduction in competition that can favor post-drought tree growth (Gómez-

Table 2. Coefficients of the Scaled Temperature, the Scaled Precipitation and Their Interaction for the Basal Area Increment (log(BAI + 1)) and the Two Spectral Indices (Eqs. 6 and 7) for the Final Models

Fixed effect	log(BAI + 1)	NDVI	NDWI
Temperature	–	–	0.0018 (0.0022)
Precipitation	0.0254 (< 0.0001)	0.0009 (0.0094)	–

–: The variable did not improve the model according to the likelihood test.
Between brackets, the results of the likelihood test (Pr(> Chisq)).

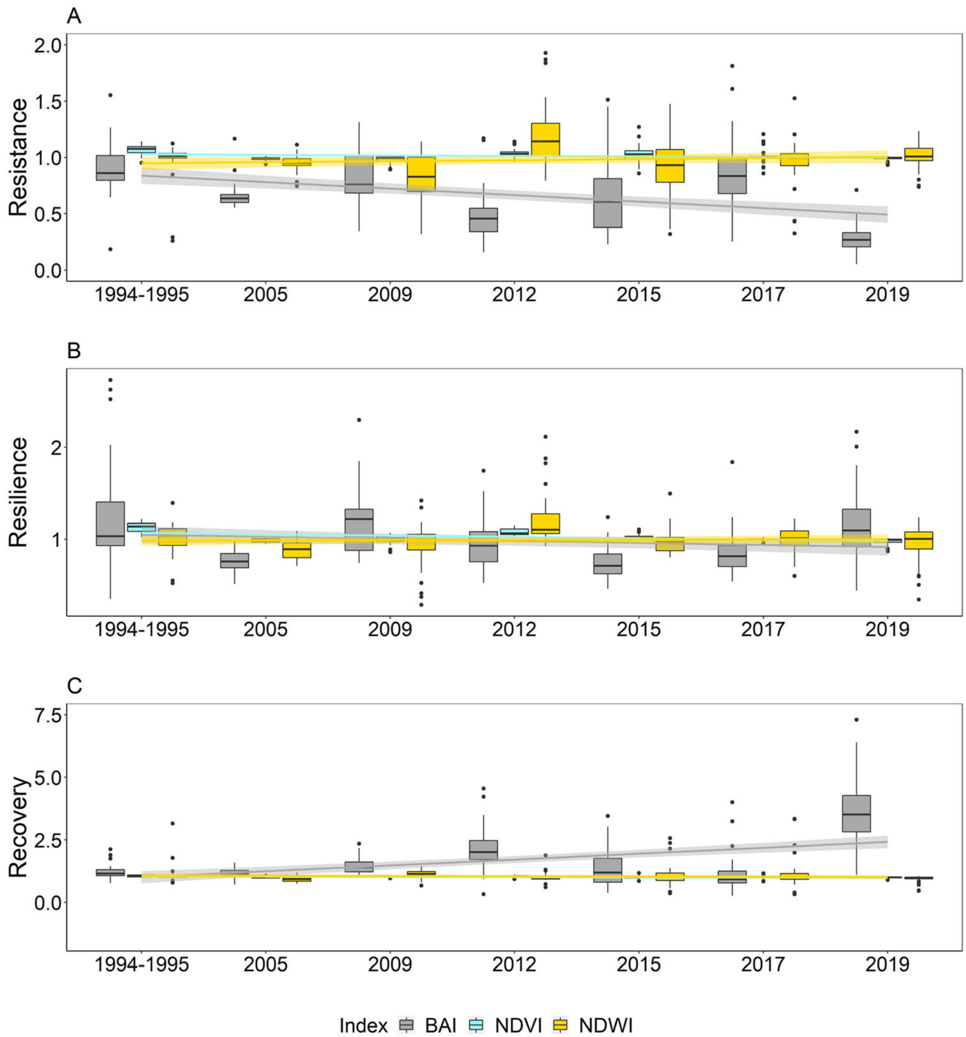

Figure 3. Boxplots and linear trends of **A** resistance, **B** resilience and **C** recovery indices for tree growth (BAI, basal area increment in mm^2), NDVI and NDWI.

Aparicio and others 2011; Moreno-Fernández and others 2013).

The drop in spectral indices occurring during the 1990s in low dieback plots could also have resulted in increased recruitment, and overstory stem turnover with resulting shrubs and herbs expansion (Rubio-Cuadrado and others 2018a; Batllori and others 2020) that attenuated the drought signal as measured by spectral indices (Ahl and others 2006; Ryu and others 2014). Under increasing aridity, companion tree species of *P. pinea* in this forest (*Q. ilex* and *J. oxycedrus*) may exhibit competitive advantage and relatively more adaptative traits to the new light and water availability environments (Mayoral and others 2015, 2016; de-Dios-García and others 2018; Férriz and others 2021; Pardos and Calama 2022). However, overstory composition did not differ significantly among dieback levels during the field survey of 2020, so we do not expect that changes in species composition over time are driving temporal patterns of spectral signals. Additionally, the basal area of other coexisting tree species was low (Table 1).

According to orthophotos interpretation and local experts (pers. comm), the external dieback symptoms (for example, canopy dieback and defoliation) were visible from 2019. The recurrent droughts from 2009 to 2020 (seven years with negative SPEI) seem to trigger the crown defoliation (dieback) and mortality processes in this forest. In concordance with our results, several studies have highlighted that recurrent droughts govern mortality and dieback phenomena in forests growing across different bioclimatic areas (Navarro-Cerrillo and others 2018; Chuste and others 2020; San-José and others 2021; Yang and others 2021).

Moreover, we observed that both tree growth and spectral indices had higher values from 2019 in currently low than moderate and high plots. This agrees with previous findings linking tree growth and spectral indices with field survey health status (Camarero and others 2015b; Sangüesa-Barreda and others 2015; Moreno-Fernández and others 2021).

In the absence of silvicultural treatments reported in our study area, the observed differences between low and moderate/high damaged plots could be due to climate and microsite conditions modulating canopy openness such as leaf shedding (Janssen and others 2021) and tree density that can lead to decreased resource availability and drought-induced responses (Brunet-Navarro and others 2016; Panayotov and others 2016; Jump and others 2017). In fact, Cavin and others (2013) observed a growth increase after a drought associated with a competition release, which could be similar to the effects of anthropogenic stand reductions via thinning (Giuggiola and others 2013; Moreno-Fernández and others 2013). However, other factors can also affect the productivity of Mediterranean pines including site conditions (Calama and others 2019), structural and functional heterogeneity (Ratcliffe and others 2016). For example, access to the water table during drought periods has been suggested as a key underlying driver of growth reduction in *P. pinea* (Mazza and Sarris 2021) and could underlie dieback on sandy or shallow soils. Regardless, we suggest that the biotic and abiotic differences in the 1990s between areas with low and moderate/high damage are leading to the current divergent dieback and mortality patterns.

Currently low damaged plots show higher tree growth since the middle 1990s (second period), almost 30 years before the emergence of currently visible dieback symptoms in 2019. This may be explained by variability in unaccounted predisposing factors (for example, site or stand conditions, soil features, genotype) making some stands more prone to drought-induced damage, and to lags between canopy and growth responses to drought with defoliation being preceded by cambial death (Pedersen 1998). All of this confirms that dendrochronology is a key tool to provide early warning measurements in forests sensitive to drought (Camarero and others 2015b, 2015a; Pellizzari and others 2016; Férriz and others 2021). In contrast to our results, other studies reported early warning signals from spectral indices (Anderegg and others 2019; Moreno-Fernández and others 2021), but in these studies the lower recovery capacity of damaged stands after the initial drought period seems to be behind the dieback (Liu and others 2021a).

Complementing Spectral Indices and Tree Growth can Better Understand Long-Term Vegetation Responses to Drought

We found differential responses for greenness and wetness indices (that is, NDVI and NDWI). Several authors investigated which type of indices are most suitable to detect forest dieback, concluding that moisture indices are preferable to those capturing only greenness (Marusig and others 2020; Moreno-Fernández and others 2021); here we did not find conclusive evidence regarding their robustness for drought-related dieback detection. However, the fact the NDWI peaked earlier (2014) than NDVI (2017) suggests that NDWI was more sensitive to the early signs of dieback than NDVI (Moreno-Fernández and others 2021). Conversely, Pascual and others (2022) reported that NDVI overperformed wetness indices in the evaluation of drought-induced mortality in a tropical *Eucalyptus* spp. forest. Similarly, Liu and others (2021b) found a faster decrease in greenness than wetness indices in response to drought in the forest-steppe ecotone, suggesting a lower chlorophyll content but stable water content to cope with drought. This variation in the performance of spectral indices among studies could reflect functionally divergent responses to seasonal drought (for example, stomatal closure, leaf shedding, etc.), and we suggest that the combined use of greenness and wetness indices is most appropriate to better understand vegetation responses to drought. Furthermore, more studies with field data are needed to disentangle what greenness and wetness indices detect.

We found low temporal correlation between spectral indices and tree growth. Previous results are inconclusive, some observing low correlations (Camarero and others 2015a; Correa-Díaz and others 2021) while other authors found coupling between tree growth data and NDVI (Vicente-Serrano and others 2016, 2020; Coulthard and others 2017; Castellaneta and others 2022). The fact that this forest is relatively open and the spectral indices also capture the signal from the understory layer (Ahl and others 2006) could be a handicap for the detection of significant relationships between remote-sensed indices and tree growth. Vicente-Serrano and others (2020), however, found stronger relationships between both data sources our study. This could be due to the fact that some species such as *P. pinea* often form open forests (see Moreno-

Fernández and others 2020 for stand attributes for *P. pinea* at the national level). Despite this, spectral indices derived from satellite data have been successfully used to monitor drought-induced forests responses (Anderegg and others 2019; Moreno-Fernández and others 2021; Pascual and others 2022), and the legacy effect of drought can be less noticeable from remotely sensed data than from tree growth series (Gazol and others 2018; Kannenberg and others 2019). In the case of photosynthesis indices, this could lead to an underestimation of drought impacts associated with bias regarding soil moisture (Stocker and others 2019). In addition, tree radial growth is a low-priority sink for resource allocation, so may be very responsive to drought (Camarero and others 2015b), as trees may rapidly reallocate resources to photosynthesis and to repair canopy damage at the expense of radial growth (Kannenberg and others 2019).

Water Stress is a Key Constraint on Tree Growth and Spectral Responses

Our findings indicate that precipitation is the main climatic variable correlated with *P. pinea* growth and spectral responses, especially for tree growth and NDVI, whereas the main constraint for NDWI was temperature. Similar to our results, several studies found that water stress and precipitation have a larger impact on *P. pinea* radial growth than temperature (Mazza and Manetti 2013; Calama and others 2019; Mazza and Sarris 2021). Shestakova and others (2021) found that radial growth of this pine is positively related to the precipitation from previous October to current May and to the temperature from previous December to current February. These authors also found a negative association between growth and May to July temperature indicating drought was magnified by higher temperature and evapotranspiration rates, and the effect of temperature on NDWI responses can be interpreted through the magnification of water demand. Overall, the heat tolerance of *P. pinea* has been suggested to be a breeding trait (Loewe Muñoz and others 2015) although, according to the above-mentioned results, the radial growth of this species could be more strongly affected by extreme drought periods.

Recurrent Droughts are Triggering the Drought-Induced Mortality

The fact that spectral resilience remained more constant over the study period than growth resilience suggests that tree growth resilience is more sensitive to drought than spectral resilience, which is in concordance with previous results (Gazol and others 2018). The greater sensitivity of tree growth than spectral indices to drought could lead to an underestimation of drought impacts if spectral indices are used alone (Stocker and others 2019). Additionally, the differential processes captured across spatial scales, that is, from the individual tree for tree growth to integrated information at the pixel scale for spectral indices, may be governing divergent interpretations of vegetation response to droughts. Tree growth measures may highlight individuals' strong responses to stress, whereas spectral information integrate vegetation responses from different species and vegetation types.

Our results indicate that during the monitoring period, tree growth resilience to drought events was relatively constant through time, whereas tree resistance strongly decreased and tree recovery increased with marked differences among drought years, depending on resilience and resistance trends. Based on resilience trends, the 2005 and 2015 droughts produced the lowest tree growth resilience. The 2005 drought is recognized to be one of the major drought episodes in the Iberian Peninsula and, resulted in widespread mortality events and a reduction in forest productivity (Galiano and others 2010; Sangüesa-Barreda and others 2015; Rodriguez-Vallejo and Navarro-Cerrillo 2019). The 2015 drought was accompanied by heatwaves (Orth and others 2016) affecting strongly tree growth in central European forests (Dietrich and others 2019) and here we show its strong effect on the tree growth resilience in Mediterranean pine forests. Based on resistance, the lowest value of resistance that occurred during the 2019 drought event could be explaining the rapid dieback process observed in the study area. Tree growth decreased in resistance over time thus suggesting that recurrent drought events could have a cumulative impact on forest health, causing crown defoliation and mortality in the long-term (Serra-Maluquer and others 2021). This also suggests that resistance is the metric most closely related and useful metric for identifying the dieback and mortality processes. In contrast, DeSoto and others (2020) argued that the drought-related mortality risk in gymnosperms is linked to low recovery capacity. Moreover, the recovery and resilience metrics for the 2019 drought should be analyzed with caution, as the post-drought period was calculated with values of one year instead of four.

Conclusions

Climate change, and, specifically, increased aridity (bringing rising temperatures and more frequent and intense dry spells) underlies the observed dieback processes in a drought-prone Mediterranean *P. pinea* forest. We compared two different organization scales—tree growth at the individual level and remote sensing at the stand level—across dieback levels.

The differential response among dieback levels could be due to a hypothesized biomass reduction (stocking) during the middle 1990s in low damaged plots evaluated through spectral indices that could have resulted in a tree growth release. In contrast, currently damaged stands did not experience a biomass reduction and, therefore, they did not show a subsequent tree growth enhancement from competitive release. The 1990s droughts initiated a divergence in trajectories of stands in our study area, with forest succession modulating the interplay of cumulative drought impacts and neighborhood competition. Our study highlights the importance of long-term retrospective multiscale analyses to disentangle mechanisms triggering and driving forest dieback. Understanding these mechanisms and monitoring post-dieback forests is critical for reducing vulnerability, forecasting changes in forest composition and structure and increasing resilience by targeting anticipatory adaptation measures.

Acknowledgments

D M-F is supported by a ''Juan de la Cierva Formación'' post-doctoral fellow (FJC2018-037870-I) from the Spanish Ministry of Science and Innovation and AV-S by the Ministry of Universities through a FPU doctoral fellowship (FPU17/03260). We acknowledge support from grants ''Data Driven Models of Forest Drought Vulnerability and Resilience across spatial and temporal Scales: Application to the Spanish Climate Change Adaptation Strategy'' (DARE: RTI2018-096884-B-C32) and FORMAL (RTI2018-096884-B-C31) from the Spanish Ministry of Science, Innovation and Universities, Spain. We also thank the support of the Community of Madrid Region under the framework of the multi-year Agreement with the University of Alcalá (Stimulus to Excellence for Permanent University Professors, EPU-INV/2020/010) and the University of Alcalá ''Ayudas para la realización de Proyectos para potenciar la Creación y Consolidación de Grupos de Investigación.'' E.R.L. was funded by a UKRI Future Leaders Fellowship (MR/T019832/1). We thank the forest rangers and the managers of Castilla La Mancha Region for their critical input and support of our activities, to especially Daniel García and Mónica Espinosa. We also thank Pedro Rebollo Orozco for his help during the field work. We recognized the comments made by two anonymous reviewers who clearly improved the quality of the study.

Funding

Open Access funding provided thanks to the CRUE-CSIC agreement with Springer Nature.

Open Access

References

Abiyu A, Mokria M, Gebrekirstos A, Bräuning A. 2018. Tree-ring record in Ethiopian church forests reveals successive generation differences in growth rates and disturbance events. Forest Ecology and Management 409:835–844.

Aguirre A, Moreno-Fernández D, Alberdi I, Hernández L, Adame P, Cañellas I, Montes F. 2022. Mapping forest site quality at national level. Forest Ecology and Management 508:120043.

Ahl DE, Gower ST, Burrows SN, Shabanov NV, Myneni RB, Knyazikhin Y. 2006. Monitoring spring canopy phenology of a deciduous broadleaf forest using MODIS. Remote Sensing of Environment 104:88–95.

Alam NM, Sharma GC, Moreira E, Jana C, Mishra PK, Sharma NK, Mandal D. 2017. Evaluation of drought using SPEI drought class transitions and log-linear models for different agro-ecological regions of India. Physics and Chemistry of the Earth, Parts A/B/C C:31–43.

Allen CD, Breshears DD, McDowell NG. 2015. On underestimation of global vulnerability to tree mortality and forest die-off from hotter drought in the Anthropocene. Ecosphere 6:129.

Anderegg WRL, Anderegg LDL, Huang C. 2019. Testing early warning metrics for drought-induced tree physiological stress and mortality. Global Change Biology 25:2459–2469.

Anderegg WRL, Trugman AT, Badgley G, Konings AG, Shaw J. 2020. Divergent forest sensitivity to repeated extreme droughts. Nature Climate Change 10:1091–1095.

Aragones D, Rodriguez-Galiano VF, Caparros-Santiago JA, Navarro-Cerrillo RM. 2019. Could land surface phenology be used to discriminate Mediterranean pine species? International Journal of Applied Earth Observation and Geoinformation 78:281–294.

Batllori E, Lloret F, Aakala T, Anderegg WRL, Aynekulu E, Bendixsen DP, Bentouati A, Bigler C, Burk CJ, Camarero JJ, Colangelo M, Coop JD, Fensham R, Floyd ML, Galiano L, Ganey JL, Gonzalez P, Jacobsen AL, Kane JM, Kitzberger T, Linares JC, Marchetti SB, Matusick G, Michaelia M, Navarro-Cerrillo RM, Pratt RB, Redmond MD, Rigling A, Ripullone F, Sangüesa-Barreda G, Sasal Y, Saura-Mas S, Suarez ML, Veblen TT, Vilà-Cabrera A, Vincke C, Zeeman B. 2020. Forest and woodland replacement patterns following drought-related mortality. Proc Natl Acad Sci U S A 117:29720–29729.

Bone C, Moseley C, Vinyeta K, Bixler RP. 2016. Employing resilience in the United States Forest Service. Land Use Policy 52:430–438.

Bottero A, D'Amato AW, Palik BJ, Bradford JB, Fraver S, Battaglia MA, Asherin LA. 2017. Density-dependent vulnerability of forest ecosystems to drought. Journal of Applied Ecology 54:1605–1614.

Bright BC, Hudak AT, Kennedy RE, Braaten JD, Henareh Khalyani A. 2019. Examining post-fire vegetation recovery with Landsat time series analysis in three western North American forest types. Fire Ecology 15:8.

Brook BW, Ellis EC, Perring MP, Mackay AW, Blomqvist L. 2013. Does the terrestrial biosphere have planetary tipping points? Trends in Ecology & Evolution 28:396–401.

Brunet-Navarro P, Sterck FJ, Vayreda J, Martinez-Vilalta J, Mohren GMJ. 2016. Self-thinning in four pine species: an evaluation of potential climate impacts. Annals of Forest Science 73:1025–1034.

Bunn AG. 2010. Statistical and visual crossdating in R using the dplR library. Dendrochronologia (verona) 28:251–258.

Buras A, Rammig A, Zang CS. 2021. The European Forest Condition Monitor: Using Remotely Sensed Forest Greenness to Identify Hot Spots of Forest Decline. Frontiers in Plant Science 12:2355.

Calama R, Conde M, De-Dios-García J, Madrigal G, Vázquez-Piqué J, Gordo FJ, Pardos M. 2019. Linking climate, annual growth and competition in a Mediterranean forest: *Pinus pinea* in the Spanish Northern Plateau. Agricultural and Forest Meteorology 264:309–321.

Camarero JJ, Franquesa M, Sangüesa-Barreda G. 2015a. Timing of drought triggers distinct growth responses in holm oak: Implications to predict warming-induced forest defoliation and growth decline. Forests 6:1576–1597.

Camarero JJ, Gazol A, Sangüesa-Barreda G, Oliva J, Vicente-Serrano SM. 2015b. To die or not to die: Early warnings of tree dieback in response to a severe drought. Journal of Ecology 103:44–57.

Castellaneta M, Rita A, Camarero JJ, Colangelo M, Ripullone F. 2022. Declines in canopy greenness and tree growth are caused by combined climate extremes during drought-induced dieback. Science of the Total Environment 813:152666.

Cavin L, Mountford EP, Peterken GF, Jump AS. 2013. Extreme drought alters competitive dominance within and between tree species in a mixed forest stand. Functional Ecology 27:1424–1435.

Chuste PA, Maillard P, Bréda N, Levillain J, Thirion E, Wortemann R, Massonnet C. 2020. Sacrificing growth and maintaining a dynamic carbohydrate storage are key processes for promoting beech survival under prolonged drought conditions. Trees - Structure and Function 34:381–394.

Correa-Díaz A, Romero-Sánchez ME, Villanueva-Díaz J. 2021. The greening effect characterized by the Normalized Difference Vegetation Index was not coupled with phenological trends and tree growth rates in eight protected mountains of central Mexico. Forest Ecology and Management 496.

Coulthard BL, Touchan R, Anchukaitis KJ, Meko DM, Sivrikaya F. 2017. Tree growth and vegetation activity at the ecosystem-scale in the eastern Mediterranean. Environmental Research Letters 12.

De Cáceres M, Martin-StPaul N, Turco M, Cabon A, Granda V. 2018. Estimating daily meteorological data and downscaling climate models over landscapes. Environmental Modelling and Software 108:186–196.

de-Dios-García J, Manso R, Calama R, Fortin M, Pardos M. 2018. A new multifactorial approach for studying intra-annual secondary growth dynamics in Mediterranean mixed forests: integrating biotic and abiotic interactions. Canadian Journal of Forest Research 48:333–44.

De Keersmaecker W, Lhermitte S, Tits L, Honnay O, Somers B, Coppin P. 2015. A model quantifying global vegetation resistance and resilience to short-term climate anomalies and their relationship with vegetation cover. Global Ecology and Biogeography 24:539–548.

DeSoto L, Cailleret M, Sterck F, Jansen S, Kramer K, Robert EMR, Aakala T, Amoroso MM, Bigler C, Camarero JJ, Čufar K, Gea-Izquierdo G, Gillner S, Haavik LJ, Hereş AM, Kane JM, Kharuk VI, Kitzberger T, Klein T, Levanič T, Linares JC, Mäkinen H, Oberhuber W, Papadopoulos A, Rohner B, Sangüesa-Barreda G, Stojanovic DB, Suárez ML, Villalba R, Martínez-Vilalta J. 2020. Low growth resilience to drought is related to future mortality risk in trees. Nature Communications 11:1–9.

Dietrich L, Delzon S, Hoch G, Kahmen A. 2019. No role for xylem embolism or carbohydrate shortage in temperate trees during the severe 2015 drought. Journal of Ecology 107:334–349.

Dobbertin M. 2005. Tree growth as indicator of tree vitality and of tree reaction to environmental stress: a review. European Journal of Forest Research 124:319–333.

Drobyshev I, Niklasson M, Ryzhkova N, Götmark F, Pinto G, Lindbladh M. 2021. Did forest fires maintain mixed oak forests in southern Scandinavia? A dendrochronological speculation. Forest Ecology and Management 482:118853.

Faraway JJ. 2006. Extending the linear model with R: generalized linear, mixed effects and nonparametric regression models.

Férriz M, Martin-Benito D, Cañellas I, Gea-Izquierdo G. 2021. Sensitivity to water stress drives differential decline and mortality dynamics of three co-occurring conifers with different drought tolerance. Forest Ecology and Management 486:118964.

Flood N. 2013. Seasonal Composite Landsat TM/ETM+ Images Using the Medoid (a Multi-Dimensional Median). Remote Sensing 5:6481–6500.

Franklin JF, Shugart HH, Harmon ME. 1987. Tree Death as an Ecological Process. BioScience 37:550–556.

Galiano L, Martínez-Vilalta J, Lloret F. 2010. Drought-Induced Multifactor Decline of Scots Pine in the Pyrenees and Potential Vegetation Change by the Expansion of Co-occurring Oak Species. Ecosystems 13:978–991.

Gao BC. 1996. NDWI—A normalized difference water index for remote sensing of vegetation liquid water from space. Remote Sensing of Environment 58:257–266.

Gazol A, Camarero JJ, Vicente-Serrano SM, Sánchez-Salguero R, Gutiérrez E, de Luis M, Sangüesa-Barreda G, Novak K, Rozas V, Tíscar PA, Linares JC, Martín-Hernández N, Martínez del Castillo E, Ribas M, García-González I, Silla F, Camisón A, Génova M, Olano JM, Longares LA, Hevia A, Tomás-Burguera M, Galván JD. 2018. Forest resilience to drought varies across biomes. Global Change Biology 24:2143–58. http://doi.wiley.com/https://doi.org/10.1111/gcb.14082. Last accessed 03/04/2021

Giuggiola A, Bugmann H, Zingg A, Dobbertin M, Rigling A. 2013. Reduction of stand density increases drought resistance in xeric Scots pine forests. Forest Ecology and Management 310:827–835.

Gómez-Aparicio L, García-Valdés R, Ruíz-Benito P, Zavala MA. 2011. Disentangling the relative importance of climate, size and competition on tree growth in Iberian forests: implications for forest management under global change. Global Change Biology 17:2400–2414.

Greenwood S, Ruiz-Benito P, Martínez-Vilalta J, Lloret F, Kitzberger T, Allen CD, Fensham R, Laughlin DC, Kattge J, Bönisch G, Kraft NJB, Jump AS. 2017. Tree mortality across biomes is promoted by drought intensity, lower wood density and higher specific leaf area. Ecology Letters 20:539–553.

Gu D, Gillespie A. 1998. Topographic normalization of Landsat TM images of forest based on subpixel Sun-canopy-sensor geometry. Remote Sensing of Environment 64:166–175.

He Z, Du J, Chen L, Zhu X, Lin P, Zhao M, Fang S. 2018. Impacts of recent climate extremes on spring phenology in arid-mountain ecosystems in China. Agricultural and Forest Meteorology 260–261:31–40.

Holmes RL. 1983. Computer-assisted quality control in tree ring dating and measurements. Tree-Ring Bull 43:69–78.

ICP Forest. 2016. International Co-operative Programme on Assessment and Monitoring of Air Pollution Effects on Forests.

Janssen T, Van Der Velde Y, Hofhansl F, Luyssaert S, Naudts K, Driessen B, Fleischer K, Dolman H. 2021. Drought effects on leaf fall, leaf flushing and stem growth in the Amazon forest: Reconciling remote sensing data and field observations. Biogeosciences 18:4445–4472.

Jump AS, Ruiz-Benito P, Greenwood S, Allen CD, Kitzberger T, Fensham R, Martínez-Vilalta J, Lloret F. 2017. Structural overshoot of tree growth with climate variability and the global spectrum of drought-induced forest dieback. Global Change Biology 23:3742–3757.

Kannenberg SA, Novick KA, Alexander MR, Maxwell JT, Moore DJP, Phillips RP, Anderegg WRL. 2019. Linking drought legacy effects across scales: From leaves to tree rings to ecosystems. Global Change Biology 25:2978–2992.

Khoury S, Coomes DA. 2020. Resilience of Spanish forests to recent droughts and climate change. Global Change Biology 26:7079–7098.

Larsson L, Larsson P. 2017. CDendro and CooRecorder.

LeBlanc DC, Nicholas NS, Zedaker SM. 1992. Prevalence of individual-tree growth decline in red spruce populations of the southern Appalachian Mountains. Forest Science 22:905–914.

Li X, Yao Y, Yin G, Peng F, Liu M. 2021. Forest resistance and resilience to 2002 drought in northern china. Remote Sensing 13:1–18.

Liu F, Liu H, Xu C, Shi L, Zhu X, Qi Y, He W. 2021a. Old-growth forests show low canopy resilience to droughts at the southern edge of the taiga. Global Change Biology.

Liu F, Liu H, Xu C, Zhu X, He W, Qi Y. 2021b. Remotely sensed birch forest resilience against climate change in the northern China forest-steppe ecotone. Ecological Indicators 125:107526.

Lloret F, Keeling EG, Sala A. 2011. Components of tree resilience: effects of successive low-growth episodes in old ponderosa pine forests. Oikos 120:1909–20. https://onlinelibrary.wiley.com/doi/full/https://doi.org/10.1111/j.1600-0706.2011.19372.x. Last accessed 11/09/2021

Loewe Muñoz V, Delard Rodríguez C, Balzarini M, Álvarez Contreras A, Navarro-Cerrillo RM. 2015. Impact of climate and management variables on stone pine (*Pinus pinea* L.) growing in Chile. Agricultural and Forest Meteorology 214–215:106–116.

Ma Z, Peng C, Zhu Q, Chen H, Yu G, Li W, Zhou X, Wang W, Zhang W. 2012. Regional drought-induced reduction in the biomass carbon sink of Canada's boreal forests. Proc Natl Acad Sci U S A 109:2423–2427.

Marqués L, Camarero JJ, Zavala MA, Stoffel M, Ballesteros-Cánovas JA, Sancho-García C, Madrigal-González J. 2021. Evaluating tree-to-tree competition during stand development in a relict Scots pine forest: how much does climate matter? Trees - Structure and Function.

Marusig D, Petruzzellis F, Tomasella M, Napolitano R, Altobelli A, Nardini A. 2020. Correlation of field-measured and remotely sensed plant water status as a tool to monitor the risk of drought-induced forest decline. Forests 11.

Mayoral C, Calama R, Sánchez-González M, Pardos M. 2015. Modelling the influence of light, water and temperature on photosynthesis in young trees of mixed Mediterranean forests. New Forests 46:485–506.

Mayoral C, Pardos M, Sánchez-González M, Brendel O, Pita P. 2016. Ecological implications of different water use strategies in three coexisting mediterranean tree species. Forest Ecology and Management 382:76–87.

Mazza G, Manetti MC. 2013. Growth rate and climate responses of *Pinus pinea* L. in Italian coastal stands over the last century. Climatic Change 121:713–725.

Mazza G, Sarris D. 2021. Identifying the full spectrum of climatic signals controlling a tree species' growth and adaptation to climate change. Ecological Indicators 130:108109.

Moreno-Fernández D, Cañellas I, Calama R, Gordo J, Sánchez-González M. 2013. Thinning increases cone production of stone pine (*Pinus pinea* L.) stands in the Northern Plateau (Spain). Annals of Forest Science 70:761–768.

Moreno-Fernández D, Cañellas I, Rubio-Cuadrado Á, Alberdi I. 2020. National scale variability in forest stand variables among regions of provenances in Spain. Annals of Forest Science 77:44.

Moreno-Fernández D, Viana-Soto A, Camarero JJ, Zavala MA, Tijerín J, García M. 2021. Using spectral indices as early warning signals of forest dieback: The case of drought-prone *Pinus pinaster* forests. Science of the Total Environment 793:148578.

Mueller-Dombois D. 1988. Forest decline and dieback — A global ecological problem. Trends in Ecology & Evolution 3:310–312.

Navarro-Cerrillo RM, Rodriguez-Vallejo C, Silveiro E, Hortal A, Palacios-Rodríguez G, Duque-Lazo J, Camarero JJ. 2018. Cumulative Drought Stress Leads to a Loss of Growth Resilience and Explains Higher Mortality in Planted than in Naturally Regenerated *Pinus pinaster* Stands. Forests 2018, Vol 9, Page 358 9:358.

Navarro-Cerrillo RM, Sánchez-Salguero R, Rodriguez C, Duque Lazo J, Moreno-Rojas JM, Palacios-Rodriguez G, Camarero JJ. 2019. Is thinning an alternative when trees could die in response to drought? The case of planted *Pinus nigra* and *P. sylvestris* stands in southern Spain. Forest Ecology and Management 433:313–324.

Ng KM, Johari J, Abdullah SAC, Ahmad A, Laja BN. 2018. Performance Evaluation of the RTK-GNSS Navigating under Different Landscape. In: 2018 18th International Conference on Control, Automation and Systems (ICCAS). pp 1424–8.

Nikinmaa L, Lindner M, Cantarello E, Jump AS, Seidl R, Winkel G, Muys B. 2020. Reviewing the Use of Resilience Concepts in Forest Sciences. Current Forestry Reports 6:61–80.

Ogaya R, Barbeta A, Başnou C, Peñuelas J. 2015. Satellite data as indicators of tree biomass growth and forest dieback in a Mediterranean holm oak forest. Annals of Forest Science 72:135–144.

Orth R, Zscheischler J, Seneviratne SI. 2016. Record dry summer in 2015 challenges precipitation projections in Central Europe. Scientific Reports 2016 6:1 6:1–8.

Pacheco A, Camarero JJ, Ribas M, Gazol A, Gutierrez E, Carrer M. 2018. Disentangling the climate-driven bimodal growth pattern in coastal and continental Mediterranean pine stands. Science of the Total Environment 615:1518–1526.

Panayotov M, Kulakowski D, Tsvetanov N, Krumm F, Berbeito I, Bebi P. 2016. Climate extremes during high competition contribute to mortality in unmanaged self-thinning Norway spruce stands in Bulgaria. Forest Ecology and Management 369:74–88.

Pardos M, Calama R. 2022. Adaptive Strategies of Seedlings of Four Mediterranean Co-Occurring Tree Species in Response to Light and Moderate Drought: A Nursery Approach. Forests 13:154.

Pascual A, Tupinambá-Simões F, Guerra-Hernández J, Bravo F. 2022. High-resolution planet satellite imagery and multi-temporal surveys to predict risk of tree mortality in tropical eucalypt forestry. Journal of Environmental Management 310:114804.

Pedersen BS. 1998. The role of stress in the mortality of Midwestern oaks as indicated by growth prior to death. Ecology 79:79–93.

Pedersen EJ, Miller DL, Simpson GL, Ross N. 2019. Hierarchical generalized additive models in ecology: An introduction with mgcv. PeerJ 2019.

Pellizzari E, Camarero JJ, Gazol A, Sangüesa-Barreda G, Carrer M. 2016. Wood anatomy and carbon-isotope discrimination support long-term hydraulic deterioration as a major cause of drought-induced dieback. Global Change Biology 22:2125–2137.

Pinheiro J, Bates D, DebRoy S, Sarkar D, R Core Team. 2020. nlme: linear and nonlinear mixed effects models. R package version 3.1–149.

Porté A, Bosc A, Champion I, Loustau D. 2000. Estimating the foliage area of Maritime pine (*Pinus pinaster* Ait.) branches and crowns with application to modelling the foliage area distribution in the crown. Annals of Forest Science 57:73–86.

R Core Team. 2021. R: A language and environment for statistical computing.

Ratcliffe S, Liebergesell M, Ruiz-Benito P, Madrigal González J, Muñoz Castañeda JM, Kändler G, Lehtonen A, Dahlgren J, Kattge J, Peñuelas J, Zavala MA, Wirth C. 2016. Modes of functional biodiversity control on tree productivity across the European continent. Global Ecology and Biogeography 25:251–262.

Reyer CPO, Brouwers N, Rammig A, Brook BW, Epila J, Grant RF, Holmgren M, Langerwisch F, Leuzinger S, Lucht W, Medlyn B, Pfeifer M, Steinkamp J, Vanderwel MC, Verbeeck H, Villela DM. 2015. Forest resilience and tipping points at different spatio-temporal scales: Approaches and challenges. Journal of Ecology 103:5–15.

Rodriguez-Vallejo C, Navarro-Cerrillo RM. 2019. Contrasting Response to Drought and Climate of Planted and Natural *Pinus pinaster* Aiton Forests in Southern Spain. Forests 2019, Vol 10, Page 603 10:603.

Rogers BM, Solvik K, Hogg EH, Ju J, Masek JG, Michaelian M, Berner LT, Goetz SJ. 2018. Detecting early warning signals of tree mortality in boreal North America using multiscale satellite data. Global Change Biology 24:2284–2304.

Roy DP, Kovalskyy V, Zhang HK, Vermote EF, Yan L, Kumar SS, Egorov A. 2016. Characterization of Landsat-7 to Landsat-8 reflective wavelength and normalized difference vegetation index continuity. Remote Sensing of Environment 185:57–70.

Rubio-Cuadrado Á, Camarero JJ, del Río M, Sánchez-González M, Ruiz-Peinado R, Bravo-Oviedo A, Gil L, Montes F. 2018a. Drought modifies tree competitiveness in an oak-beech temperate forest. Forest Ecology and Management 429:7–17.

Rubio-Cuadrado Á, Camarero JJ, del Río M, Sánchez-González M, Ruiz-Peinado R, Bravo-Oviedo A, Gil L, Montes F. 2018b. Long-term impacts of drought on growth and forest dynamics in a temperate beech-oak-birch forest. Agricultural and Forest Meteorology 259:48–59.

Rubio-Cuadrado Á, Gómez C, Rodríguez-Calcerrada J, Perea R, Gordaliza GG, Camarero JJ, Montes F, Gil L. 2021. Differential response of oak and beech to late frost damage: an integrated analysis from organ to forest. Agricultural and Forest Meteorology 297:108243.

Ryu Y, Lee G, Jeon S, Song Y, Kimm H. 2014. Monitoring multi-layer canopy spring phenology of temperate deciduous and evergreen forests using low-cost spectral sensors. Remote Sensing of Environment 149:227–238.

Salmon Y, Dietrich L, Sevanto S, Hölttä T, Dannoura M, Epron D. 2019. Drought impacts on tree phloem: from cell-level responses to ecological significance. Tree Physiology 39:173–191.

Sánchez-Pinillos M, D'Orangeville L, Yan B, Comeau P, Wang J, Taylor AR, Kneeshaw D. 2021. Sequential droughts: a silent trigger of boreal forest mortality. Global Change Biology.

Sangüesa-Barreda G, Camarero JJ, Oliva J, Montes F, Gazol A. 2015. Past logging, drought and pathogens interact and contribute to forest dieback. Agricultural and Forest Meteorology 208:85–94.

San-José M, Werden L, Peterson CJ, Oviedo-Brenes F, Zahawi RA. 2021. Large tree mortality leads to major aboveground biomass decline in a tropical forest reserve. Oecologia 197:795–806.

Schielzeth H. 2010. Simple means to improve the interpretability of regression coefficients. Methods in Ecology and Evolution 1:103–113.

Seifert T, Meincken M, Odhiambo BO. 2017. The effect of surface fire on tree ring growth of *Pinus radiata* trees. Annals of Forest Science 74:34.

Serra-Maluquer X, Granda E, Camarero JJ, Vilà-Cabrera A, Jump AS, Sánchez-Salguero R, Sangüesa-Barreda G, Imbert JB, Gazol A. 2021. Impacts of recurrent dry and wet years alter long-term tree growth trajectories. Journal of Ecology 109:1561–1574.

Shestakova TA, Mutke S, Gordo J, Camarero JJ, Sin E, Pemán J, Voltas J. 2021. Weather as main driver for masting and stem growth variation in stone pine supports compatible timber and nut co-production. Agricultural and Forest Meteorology 298–299:108287.

Soenen SA, Peddle DR, Coburn CA. 2005. SCS+C: A modified sun-canopy-sensor topographic correction in forested terrain. IEEE Transactions on Geoscience and Remote Sensing 43:2148–2159.

Stocker BD, Zscheischler J, Keenan TF, Prentice IC, Seneviratne SI, Peñuelas J. 2019. Drought impacts on terrestrial primary production underestimated by satellite monitoring. Nature Geoscience 2019 12:4 12:264–70.

Tucker CJ. 1979. Red and photographic infrared linear combinations for monitoring vegetation. Remote Sensing of Environment 8:127–150.

Valeriano C, Gazol A, Colangelo M, Camarero JJ. 2021. Drought Drives Growth and Mortality Rates in Three Pine Species under Mediterranean Conditions. Forests 12:1700.

Vicente-Serrano SM, Beguería S, López-Moreno JI. 2010. A multiscalar drought index sensitive to global warming: The standardized precipitation evapotranspiration index. Journal of Climate 23:1696–1718.

Vicente-Serrano SM, Camarero JJ, Olano JM, Martín-Hernández N, Peña-Gallardo M, Tomás-Burguera M, Gazol A, Azorin-Molina C, Bhuyan U, El Kenawy A. 2016. Diverse relationships between forest growth and the Normalized Difference Vegetation Index at a global scale. Remote Sensing of Environment 187:14–29.

Vicente-Serrano SM, Lopez-Moreno J-I, Beguería S, Lorenzo-Lacruz J, Sanchez-Lorenzo A, García-Ruiz JM, Azorin-Molina C, Morán-Tejeda E, Revuelto J, Trigo R, Coelho F, Espejo F. 2014. Evidence of increasing drought severity caused by temperature rise in southern Europe. Environmental Research Letters 9:044001.

Vicente-Serrano SM, Martín-Hernández N, Camarero JJ, Gazol A, Sánchez-Salguero R, Peña-Gallardo M, el Kenawy A, Domínguez-Castro F, Tomas-Burguera M, Gutiérrez E, de Luis M, Sangüesa-Barreda G, Novak K, Rozas V, Tíscar PA, Linares JC, del Castillo EM, Ribas M, García-González I, Silla F, Camisón A, Génova M, Olano JM, Longares LA, Hevia A, DiegoGalván J. 2020. Linking tree-ring growth and satellite-derived gross primary growth in multiple forest biomes. Temporal-scale matters. Ecological Indicators 108:105753. https://doi.org/10.1016/j.ecolind.2019.105753.

Vicente-Serrano SM, Tomas-Burguera M, Beguería S, Reig F, Latorre B, Peña-Gallardo M, Luna MY, Morata A, González-Hidalgo JC. 2017. A High Resolution Dataset of Drought Indices for Spain. Data (Basel) 2:22.

Visser H. 1995. Note on the Relation Between Ring Widths and Basal Area Increments. Forest Science 41:297–304.

Wood SN. 2003. Thin-Plate Regression Splines. Journal of the Royal Statistical Society (B) 65:95–114.

Wood SN. 2006. Generalized Additive Models: an Introduction with R. United States of America: CRC Press.

Wood SN. 2017. Generalized Additive Models: An Introduction with R. Second. Chapman and Hall/CRC

Wu S, Wang J, Yan Z, Song G, Chen Y, Ma Q, Deng M, Wu Y, Zhao Y, Guo Z, Yuan Z, Dai G, Xu X, Yang X, Su Y, Liu L, Wu J. 2021. Monitoring tree-crown scale autumn leaf phenology in a temperate forest with an integration of PlanetScope and drone remote sensing observations. ISPRS Journal of Photogrammetry and Remote Sensing 171:36–48.

Yamaguchi DK. 1991. A simple method for cross-dating increment cores from living trees. Canadian Journal of Forest Research 21:414–416.

Yang S, Spetich MA, Fan Z. 2021. Spatiotemporal dynamics and risk factors of oak decline and Mortality in the Missouri Ozarks of the United States based on repeatedly measured FIA data. Forest Ecology and Management 502:119745.

Zhao K, Hu T, Li Y. 2019a. Rbeast: Bayesian Change-Point Detection and Time Series Decomposition.

Zhao K, Wulder MA, Hu T, Bright R, Wu Q, Qin H, Li Y, Toman E, Mallick B, Zhang X, Brown M. 2019b. Detecting change-point, trend, and seasonality in satellite time series data to track abrupt changes and nonlinear dynamics: A Bayesian ensemble algorithm. Remote Sensing of Environment 232:111181.

Zhou Y, Yi Y, Jia W, Cai Y, Yang W, Li Z. 2020. Applying dendrochronology and remote sensing to explore climate-drive in montane forests over space and time. Quaternary Science Reviews 237:106292.

Zhu X, Liu D. 2015. Improving forest aboveground biomass estimation using seasonal Landsat NDVI time-series. ISPRS Journal of Photogrammetry and Remote Sensing 102:222–231.

Zuur A, Ieno EN, Walker N, Saveliev AA, Smith GM. 2009. Mixed effects models and extensions in ecology with R. New York: Springer.